The *Arabidopsis thaliana MND1* homologue plays a key role in meiotic homologous pairing, synapsis and recombination

Claudia Kerzendorfer[1,2,*], Julien Vignard[3,*], Andrea Pedrosa-Harand[1], Tanja Siwiec[1], Svetlana Akimcheva[2], Sylvie Jolivet[3], Robert Sablowski[4], Susan Armstrong[5], Dieter Schweizer[1,2], Raphael Mercier[3,‡] and Peter Schlögelhofer[1,‡]

[1]Department of Chromosome Biology, Max F. Perutz Laboratories, University of Vienna, A-1030 Vienna, Austria
[2]Gregor Mendel Institute of Molecular Plant Biology, Austrian Academy of Sciences, A-1030 Vienna, Austria
[3]Station de Génétique et d'Amélioration des Plantes, Institut National de la Recherche Agronomique, 78026 Versailles CEDEX, France
[4]Department of Cell and Developmental Biology, John Innes Centre, Norwich, NR4 7UH, UK
[5]School of Bioscience, University of Birmingham, Birmingham, B15 2TT, UK
*These authors contributed equally to this work
‡Authors for correspondence (e-mail: rmercier@versailles.inra.fr; peter.schloegelhofer@univie.ac.at)

Accepted 1 March 2006
Journal of Cell Science 119, 2486-2496 Published by The Company of Biologists 2006
doi:10.1242/jcs.02967

Summary

Mnd1 has recently been identified in yeast as a key player in meiotic recombination. Here we describe the identification and functional characterisation of the *Arabidopsis* homologue, *AtMND1*, which is essential for male and female meiosis and thus for plant fertility. Although axial elements are formed normally, sister chromatid cohesion is established and recombination initiation appears to be unaffected in mutant plants, chromosomes do not synapse. During meiotic progression, a mass of entangled chromosomes, interconnected by chromatin bridges, and severe chromosome fragmentation are observed. These defects depend on the presence of SPO11-1, a protein that initiates recombination by catalysing DNA double-strand break (DSB) formation. Furthermore, we demonstrate that the AtMND1 protein interacts with AHP2, the *Arabidopsis* protein closely related to budding yeast Hop2. These data demonstrate that AtMND1 plays a key role in homologous synapsis and in DSB repair during meiotic recombination.

Supplementary material available online at
http://jcs.biologists.org/cgi/content/full/119/12/2486/DC1

Key words: *Arabidopsis*, Meiosis, Recombination, Synapsis

Introduction

Meiosis is the specialised cell division that sexually reproducing organisms undergo in order to reduce the chromosome number by half before gamete formation. Most cells of diploid organisms contain two corresponding – homologous – sets of chromosomes, one from the mother and one from the father. Both sets are replicated, recombined and subsequently distributed to four daughter cells in two successive rounds of cell division during the process of meiosis. During the first division (meiosis I), pairs of replicated homologous chromosomes are separated, whereas during the second division (meiosis II), it is the sister chromatids that are separated. Before homologous chromosomes are separated at meiosis I, they associate in pairs, synapse during prophase – culminating in the formation of a tripartite proteinaceous structure called the synaptonemal complex (SC) – and homologous recombination occurs, resulting in both crossover and non-crossover (or gene conversion) events. Homologous recombination results in the formation of chromosomes consisting of both paternal and maternal DNA sequences and consequently contributes to the genetic diversity of the four meiotic products (reviewed by Page and Hawley, 2003; Zickler and Kleckner, 1999).

Homologous recombination in meiosis proceeds by specialised repair of DNA DSBs, generated by the type-II topoisomerase-like enzyme Spo11 (Bergerat et al., 1997; Keeney et al., 1997). In many species, including *Saccharomyces cerevisiae* and *Arabidopsis thaliana*, the formation of the SC depends on meiotic recombination initiation by Spo11 (Grelon et al., 2001; Henderson and Keeney, 2004) and it is believed that the SC starts to form at these sites of broken DNA (Agarwal and Roeder, 2000; de Vries et al., 2005).

The DSB processing mechanisms that eventually lead to crossover and non-crossover events have been deciphered at the molecular level, primarily in yeast. DSB repair, which preferentially uses the homologous chromosome as a template, is mediated by two recombinases, Rad51 and Dmc1 (reviewed by Okada and Keeney, 2005). Following DNA DSB formation and resection, Rad51 is loaded onto single-stranded DNA (ssDNA). Rad51 has a role in both somatic and meiotic recombination, whereas the closely related strand-exchange factor Dmc1 is exclusively loaded onto ssDNA during meiosis (Pâques and Haber, 1999). Dmc1 physically interacts with Tid1/Rdh54 (Dresser et al., 1997), which mediates loading and is required, together with other factors, for inter-homologue

recombination (but not inter-sister recombination) (Schwacha and Kleckner, 1997). One such factor is Hop2, which is indispensable for homologous recombination and inter-homologue bias during meiosis (Tsubouchi and Roeder, 2002). Hop2 requires the binding of Mnd1 to be functional (Chen et al., 2004). The budding yeast *Mnd1* gene was identified in a screen for genes expressed early during meiosis (Rabitsch et al., 2001). Mutation of *Mnd1* leads to meiotic arrest owing to hyper-resected DSBs and aberrant synapsis (Zierhut et al., 2004), a phenotype similar to that of *hop2* mutants (Gerton and DeRisi, 2002; Leu et al., 1998; Tsubouchi and Roeder, 2002), leading to meiotic arrest owing to hyper-resected DSBs and aberrant synapsis (Zierhut et al., 2004). Furthermore, Mnd1 is a multicopy suppressor of a *hop2ts* mutation. Analyses of Hop2 in organisms other than budding yeast, such as fission yeast, mouse and *Arabidopsis* have underlined its importance for the regular processing of DSBs and synapsis between homologues (Nabeshima et al., 2001; Petukhova et al., 2003; Schommer et al., 2003). In vitro analysis of purified yeast Hop2 and Mnd1 proteins, has established that the heterodimer improves Dmc1 D-loop formation activity (Chen et al., 2004). In vitro data obtained from purified mouse proteins demonstrate that only Hop2 possesses strand invasion activity, that is inhibited by Mnd1, and that the Hop2-Mnd1 heterodimer stimulates the strand invasion activity of Dmc1 and Rad51 up to 35-fold (Petukhova et al., 2005). The current model of Hop2-Mnd1 function views the latter protein as a kind of match-maker, ensuring that the Hop2 strand invasion capacity is only elicited in the context of Dmc1 and/or Rad51. Moreover, it assumes that the Mnd1-Hop2 heterodimer and Dmc1 promote DSB repair specifically when homologous chromosomes are available as repair templates. If meiotic inter-homologue bias is disrupted by mutation of inter-homologue bias-determining factors such as Hop1 or Red1, *mnd1* mutants can repair meiotic DSBs, by using the sister chromatid as a template (Zierhut et al., 2004).

Mnd1 is present in the genomes of several organisms (Gerton and DeRisi, 2002; Zierhut et al., 2004) but so far has only been functionally characterised in budding and fission yeasts (Saito et al., 2004; Tsubouchi and Roeder, 2002). Purified Mnd1 protein from mouse has been biochemically studied in vitro (Petukhova et al., 2005), but no mutant has been generated. We present the first functional characterisation of an *Mnd1* homologue in a higher eukaryote, *AtMND1* from *A. thaliana*. We demonstrate that *AtMND1* is essential for male and female meiosis, and that mutation of this gene leads to sterility. Although axial elements are formed normally, sister chromatid cohesion is established and recombination initiation appears to be unaffected (according to the formation of RAD51 foci) in mutant plants, chromosomes do not synapse. A mass of entangled chromosomes, interconnected by chromatin bridges and exhibiting severe chromosome fragmentation were observed during meiotic progression. This fragmentation depends on the presence of the SPO11-1 protein. These data demonstrate that AtMND1 is involved in meiotic recombination and repair, and that its absence leads to unprocessed or abnormally repaired meiotic DSBs. Using as yeast two-hybrid (Y2H) assay, we show that AtMND1 interacts with AHP2, the *A. thaliana* homologue of Hop2. We conclude that AtMND1 associates with AHP2 and that together they act as key proteins in meiotic recombination, a feature apparently conserved from yeasts to higher eukaryotes.

Results

Characterisation of the *AtMND1* gene

Zierhut et al. (Zierhut et al., 2004) present predicted homologues of the *Saccharomyces cerevisiae Mnd1* gene found in BLAST searches (Altschul et al., 1997) against GenBank. Genes were found in *Encephalozoon cuniculi*, *Schizosaccharomyces pombe*, *A. thaliana*, *Mus musculus* and *Homo sapiens*. An *Mnd1* gene homologue has not been found in either *Drosophila melanogaster* or *Caenorhabditis elegans* (Gerton and DeRisi, 2002), both of which differ from other organisms with respect to the initial stages of meiosis. The *A. thaliana* gene homologue of the yeast *Mnd1* gene has been named *AtMND1* (At4g29170). It shares 43% identity to the human, 42% to the mouse, 38% to the *S. pombe* and 26% to the *S. cerevisiae* gene homologues. *AtMND1* has ten exons; its mRNA, including 5′ and 3′ UTRs, is 994 bp in length as determined by RACE (GenBank accession number: DQ248000), and its ORF is 693 bp in length (Fig. 1A). We obtained the *AtMND1* cDNA sequence from the *Arabidopsis* Biological Resource Center (Yamada et al., 2003) and confirmed its identity by sequencing.

Molecular and morphological characterisation of the *Atmnd1* mutant

An insertion mutant line (SALK_110052), carrying a T-DNA insertion in the *AtMND1* gene region, was identified in the Salk Institute Genomic Analysis Laboratory T-DNA collection (Alonso et al., 2003). In Fig. 1A, the position of the T-DNA insertion within the seventh intron of the *AtMND1* gene is shown. PCR amplification of T-DNA border regions was accomplished by combining primers from the left border of the T-DNA with gene-specific primers. Sequencing of these PCR products revealed, that the T-DNA insert has two left borders and that a 85-bp fragment of the seventh intron of the *AtMND1* sequence is deleted in the mutant plant (Fig. 1B). DNA gel blot analysis was performed to characterise the nature of the T-DNA insertion. DNA from individual plants was extracted, digested with the endonuclease *Hin*dIII, separated, and blotted. Detection of the *AtMND1* sequence was performed with a probe corresponding to the entire genomic region of *AtMND1*. The blot shows the expected bands for wild-type (+/+) (0.8 kb band; 3.2 kb band), heterozygous (+/–) (0.8 kb band; 2.2/2.3 kb bands; 3.2 kb band) and homozygous mutant plants (–/–) (2.2/2.3 kb bands; 3.2 kb band) (Fig. 1A,C). Re-probing the blot with a probe derived from the T-DNA, indicated that there is only one T-DNA integration locus, which consists of multiple T-DNA repeats (data not shown). Plant genotypes were routinely determined by multiplex PCR, combining primers M2, M3 and LBa1 in one reaction (Fig. 1A,D). The expected DNA fragment lengths for wild-type and mutant alleles are ~0.9 kb and ~1.3 kb, respectively. Wild-type and homozygous mutant plants, selected by PCR, were analysed for expression of the *AtMND1* gene by RT-PCR. The cDNA of *AtMND1* (693 bp) was only detected in wild-type samples. By contrast, the *ACTIN* cDNA control (390 bp) was detected in mutant and wild-type samples (Fig. 1E). Expression of *AtMND1* was found in buds, leaves and shoots (Fig. 1E). This finding

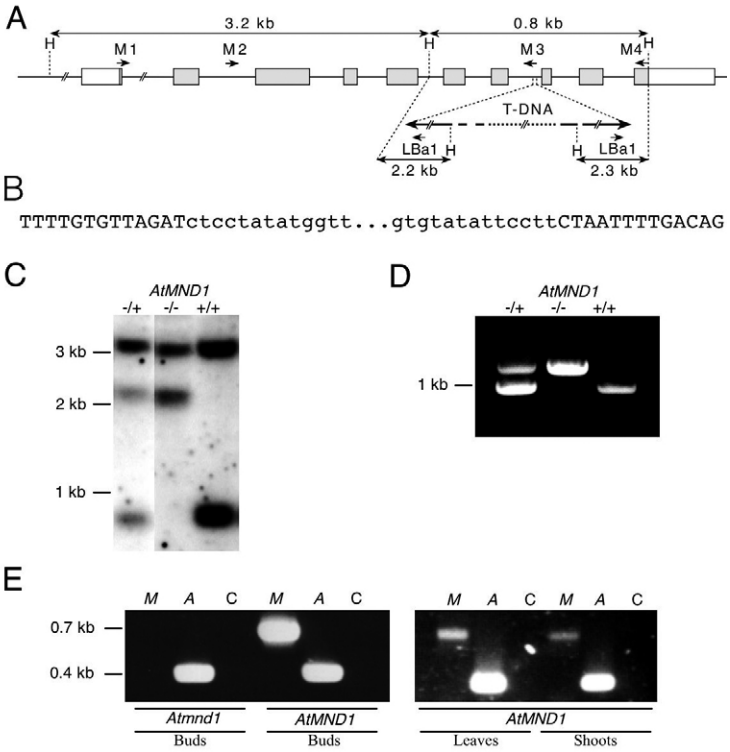

Fig. 1. Molecular analysis of the *AtMND1* T-DNA insertion mutant. (A) Schematic representation of the *Atmnd1* mutant allele with the T-DNA insertion. The T-DNA insertion site as well as the orientation of left borders are indicated. The boxes represent exons, with UTRs in white and cDNA sequence in grey. The positions of the primers (arrows) and *Hin*dIII restriction sites (H) are marked. Expected DNA fragments after digestion are indicated by double arrows. (B) DNA sequence of the junction between T-DNA and genomic DNA. Capital letters indicate genomic sequences adjacent to the borders of the T-DNA. Lowercase letters indicate the deleted 85-bp genomic region. (C) DNA gel blot hybridisation of *Hin*dIII-digested genomic DNA with a genomic *AtMND1* probe results in the production of ~0.8 kb and ~3.2 kb bands for wild-type (+/+), ~0.8 kb, ~2.2/2.3 kb and ~3.2 kb bands for heterozygous (+/–) and ~2.2/2.3 kb and ~3.2 kb for homozygous (–/–) mutant plants. (D) PCR assay to distinguish wild-type, heterozygous and homozygous mutant plants. Primers M2, M3 and LBa1 were used in the same PCR reaction. (E) RT-PCR experiment to analyse the expression of *AtMND1*. The *AtMND1* transcript (M) was detected in various wild-type tissues but not in the Atmnd1 mutant line. Amplification of the *ACTIN* (A) transcripts was used as a control. C represents a control experiment with the corresponding RNA as template in the PCR amplification reaction, using primers directed against *ACTIN*. The expected band size for *AtMND1* cDNA is ~0.7 kb and for *ACTIN* cDNA is ~0.4 kb.

is consistent with publicly available microarray data (http://www.genevestigator.ethz.ch).

Plants heterozygous for the *Atmnd1* mutation were indistinguishable from wild-type plants and self-fertilisation produced homozygous mutants in the expected 3:1 ratio. Homozygous *Atmnd1* mutants do not have any obvious growth aberrations during vegetative development. The mutants germinate at the same time as wild-type plants and develop at the same rate. Rosette leaves looked normal and bolting was not delayed. Inflorescences also looked normal but none of the siliques of *Atmnd1* plants elongated. Whereas senescent shoots of wild-type plants had long siliques and a terminal inflorescence that ceased to develop further, *Atmnd1* mutant plants possess only very short siliques and an inflorescence that produces flowers for a much longer time period than wild-type plants. The short siliques of *Atmnd1* plants produced only 0.033 seeds/silique (n=4930) (Fig. 2A). About half of these seeds germinated (0.019% seeds/silique), but very few formed a plant body. None of these plants had a normal morphology and none produced seeds (data not shown).

To confirm that the *Atmnd1* mutation caused the sterility phenotype, heterozygous *Atmnd1* mutant plants were transformed with a T-DNA construct containing a genomic DNA fragment, harbouring the *AtMND1* gene and its putative promoter region. Transformants were selected and simultaneously screened with PCR for the presence of the *Atmnd1* mutation. Four individual transformants, containing the complementing T-DNA and harbouring the *Atmnd1* mutant allele either in heterozygous or homozygous configuration were analysed for the production of sterile offspring plants. All offspring that contained the complementing T-DNA (n=108) were fertile, indicating complete reversion of the sterility phenotype in the presence of a genomic copy of *AtMND1* (Fig. 2A).

Male and female meiosis is severely disrupted in *Atmnd1* mutants

Both the sterility observed in our *Atmnd1* mutant plants as well the results of Mnd1 analyses in other organisms suggested that there is a meiotic defect in *A. thaliana Atmnd1* mutants. The viability of pollen grains, the products of male meiosis, can easily be visualised by Alexander staining (Alexander, 1969). Wild-type anthers contain many mature and viable pollen grains, as visualised by the red staining of the cytoplasm (Fig. 2B). By contrast, *Atmnd1* mutant plants develop anthers that are devoid of regular pollen grains. The aborted pollen grains, visualised by the green counter-stain of the pollen wall, are generally smaller and variable in size (Fig. 2B). 93% of all *Atmnd1* anthers contained no viable pollen grains, 6% contained one and 1% contained two viable pollen grains (n=81). All of these viable pollen grains looked bigger and non-regular in shape (supplementary material Fig. S1G-J).

We investigated the behaviour of meiotic chromosomes in *Atmnd1* mutants and in wild-type plants, by means of a meiocyte spreading technique (Fig. 3). In wild-type meiocytes, the ten *A. thaliana* chromosomes appear as thread-like structures in leptotene (Fig. 3A), undergo synapsis in zygotene (Fig. 3B) and are fully synapsed along their entire lengths, at pachytene (Fig. 3C). After the disappearance of the SC in diplotene (Fig. 3D), the resulting five bivalents condensed, revealing the presence of chiasmata in diakinesis (Fig. 3E,F). The bivalents assembled at the metaphase I plate (Fig. 3G) and segregated homologues at anaphase I (Fig. 3H). During meiosis II, the second round of segregation leads to the formation of four sets of five chromatids (Fig. 3I).

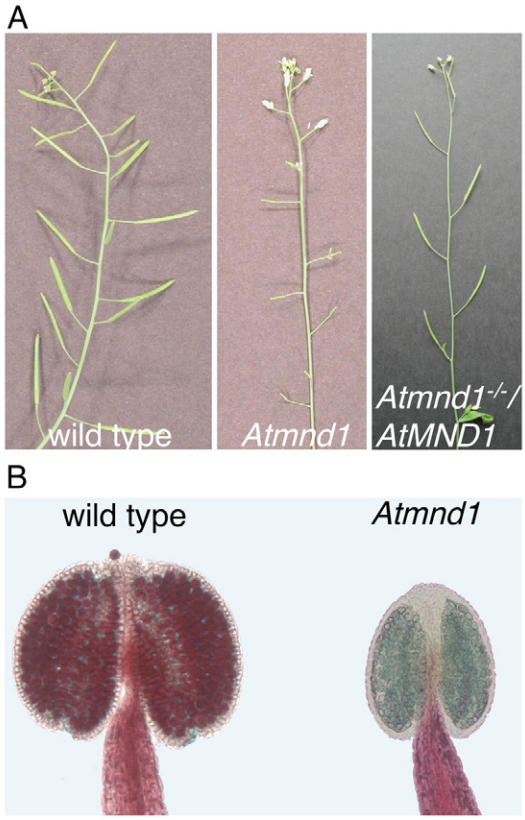

Fig. 2. *Atmnd1* mutant plants develop short siliques and no regular pollen grains. (A) *Atmnd1* plants look like wild-type plants, except that they have shorter and empty siliques. The left panel shows a stem with full-grown siliques of a wild-type plant (wt). The middle panel shows the stem of an *Atmnd1* plant of the same age, which failed to develop siliques (*Atmnd1*). The right panel shows an *Atmnd1* homozygous mutant plant, transformed with a wild-type copy of the genomic *AtMND1* region and showing restored fertility. (B) Anthers of wild-type (left panel) and *Atmnd1* (right panel) plants stained according to Alexander (Alexander, 1969). The purple-stained cytoplasm indicates viable pollen grains. *Atmnd1* plants did not develop regular pollen grains.

In *Atmnd1* meiocytes, the first step of prophase I, leptotene, appeared similar to that in wild-type meiocytes (compare Fig. 3J with 3A). The first observable defect in *Atmnd1* meiocytes was the absence of typical zygotene and pachytene stages, during which synapsis normally occurs. Instead, we observed zygotene-like (compare Fig. 3K with 3B) and pachytene-like stages (compare Fig. 3L to 3C), with a clear absence of extended synapsis. Some alignment seemed to occur at this stage but the short stretches of associated chromosome axes observed, could have been formed by chance during the spreading procedure. In any case, it became clear from subsequent stages that synapsis, even if initiated, did not extend to completion in the *Atmnd1* mutant. Subsequently, chromosomes condensed progressively and altered chromosome structures during early diakinesis-like stage (Fig. 3M) and diakinesis-like stage (compare Fig. 3N with 3F). DNA masses erratically linked by chromatin bridges became visible. Instead of five separated bivalents, maintained by chiasmata, an entangled mass of chromosomes was observed at the metaphase-I-like stage (compare Fig. 3O with 3G). At anaphase I, the chromosome mass separated and chromosome fragments appeared (Fig. 3P). During the second meiotic division, chromosome fragmentation was visible at the metaphase-II-like stage (Fig. 3Q) and became more pronounced at the telophase-II-like stage (Fig. 3R).

As meiotic defects can have different consequences for male and female meiosis in *Arabidopsis* (Mercier et al., 2001), we investigated female meiosis and gametophyte development in *Atmnd1* plants. We found that 2.4% of fully grown ovules in *Atmnd1*$^{-/-}$ mutants contained apparently normal embryo sacs, 2.8% contained an embryo sac blocked during mitotic divisions and 94.8% contained a degenerated or a single nucleus embryo sac (n=611) (supplementary material Fig. S1A-F). We pollinated *Atmnd1*$^{-/-}$ mutants with wild-type pollen and found 2.2% seed formation (1.08 seeds/silique, n=25) when compared with the wild type (50 seeds/silique). Only 0.68 seeds/silique were viable, leading to an overall fertility of 1.4%. This indicates that female meiosis is less affected than male meiosis. The cytological defects observed were similar to those seen in male meiosis (Fig. 4). Typical pachytene stages were not observed (compare Fig. 4D with 4A), an entangled chromosome mass instead of five bivalents was formed at metaphase I-like stages (compare Fig. 4E with 4B) and chromosome fragmentation appeared at anaphase I-like stages (compare Fig. 4F with 4C).

Defective pairing and non-disjunction of chromosomes in *Atmnd1* mutants

Chromosomes undergo pairing during meiosis in wild-type plants, with telomeres clustering during leptotene at the nucleolus and associating in pairs before recombination-mediated alignment of chromosomes (Armstrong et al., 2001). In zygotene, FISH signals corresponding to regions adjacent to telomeres are paired or are in close proximity (Fig. 5A, red signal corresponds to a sub-telomeric region of chromosome 2), whereas interstitial chromosomal regions are paired or not, depending on the progression of zygotene (Fig. 5A, green signal corresponds to an interstitial region of chromosome 1). In pachytene, chromosome pairing is completed and only one signal can be seen for each FISH probe (Fig. 5B). Homologous chromosomes separate during anaphase I, a process that requires sister-chromatid cohesion to be lost in arm regions (reviewed by Watanabe, 2004). Therefore, a pair of FISH signals, corresponding to the two sister-chromatids, are frequently seen on each homologue (Fig. 5C). In *Atmnd1* mutants, no pairing of homologues is observed. In zygotene, the sub-telomeric regions are sometimes paired or in close proximity to each other (red signal, Fig. 5D), but no pairing was ever detected during meiotic progression for the two FISH probes analyzed (pachytene-like stage shown in Fig. 5E). At the anaphase-I-like stage (Fig. 5F), chromosome fragmentation and chromosome bridges were visible and the FISH signals indicate that homologous chromosomes 1 and 2 do not regularly segregate.

Chromosome entanglement and fragmentation observed in *Atmnd1* mutants depends on SPO11-1

To determine whether SPO11 function is involved in the chromosome fragmentation observed in prophase I in *Atmnd1* mutant plants, we generated *Atmnd1 spo11-1* double mutants. Although *A. thaliana* possesses three *SPO11* homologues,

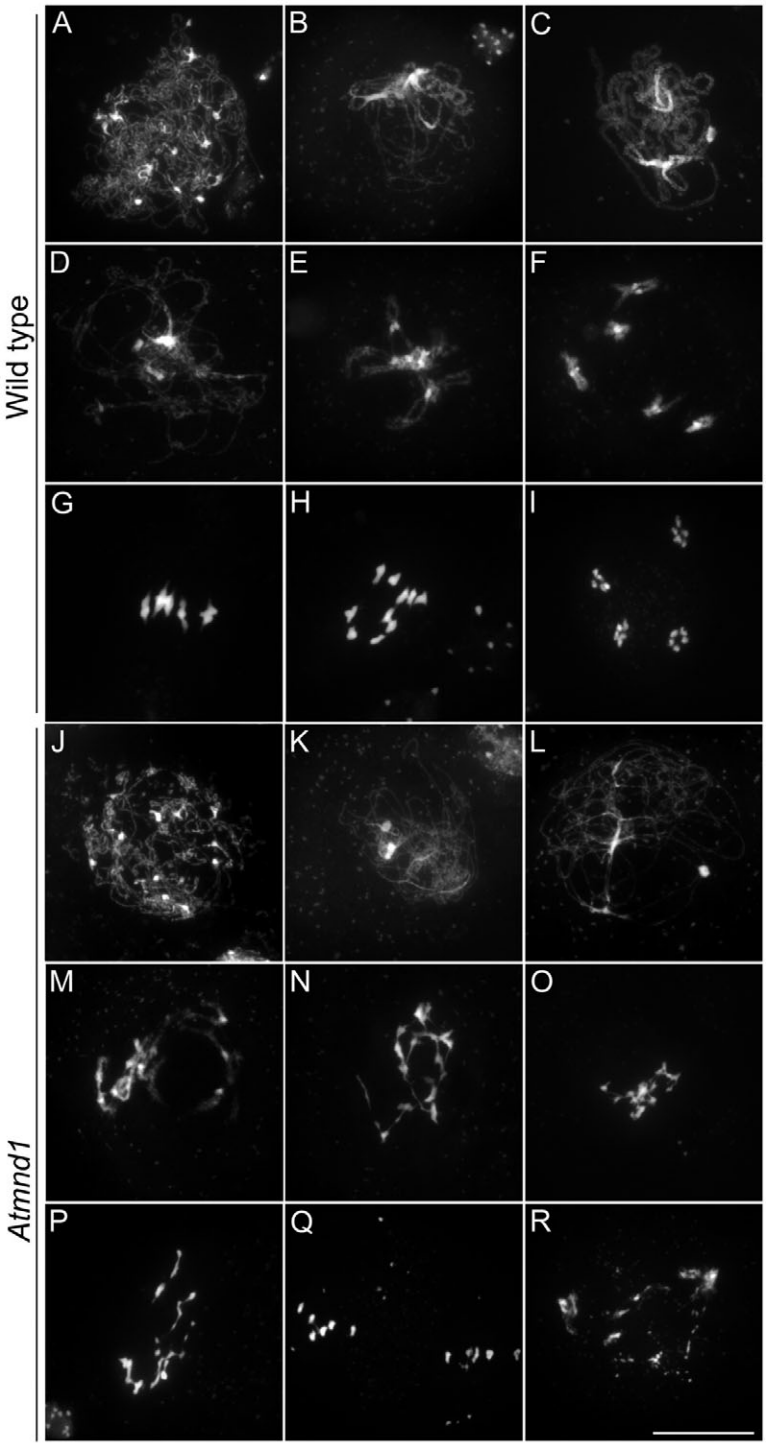

Fig. 3. Male meiosis is severely disrupted in *Atmnd1* mutants. Meiosis in wild-type *A. thaliana*: (A) leptotene, (B) zygotene, (C) pachytene, (D) diplotene, (E) early diakinesis, (F) diakinesis, (G) metaphase I, (H) anaphase I, (I) telophase II. Disrupted male meiosis in the *Atmnd1* mutant: (J) leptotene, indistinguishable from the wild type. (K) Zygotene-like stage. (L) Pachytene-like stage. The mutant failed to go through typical zygotene and pachytene stages, displaying no pairing and synapsis of chromosomes. (M) Early diakinesis-like stage, (N) late diakinesis-like stage and (O) metaphase-I-like stage show entangled chromosomes interconnected by chromatin bridges. (P) Progression through anaphase I with stretched chromatin and limited chromosome fragmentation. (Q) Metaphase II-like stage with chromosome fragments. (R) Late-anaphase-II-like stage with severe chromosome fragmentation. Chromosomes are stained with DAPI. Bar, 10 μm.

SPO11-1 is probably the only meiotic protein of the three *SPO11* proteins (Grelon et al., 2001; Yin et al., 2002) (M. Grelon, INRA IJPB, Versailles, France, personal communication). Meiotic progression of *spo11-1* mutants was compared with *Atmnd1 spo11-1* double mutants (Fig. 6). Leptotene stages (not shown) were comparable with wild-type meiocytes. However, neither single nor double mutants displayed paired chromosomes; thus, only failed zygotenes (Fig. 6A,G) and only unsynapsed chromosomes of a pachytene-like stage (Fig. 6B,H) were observed. During diakinesis (Fig. 6C,I), chromosomes condensed and ten univalents were visible which then, after alignment at metaphase I, were randomly distributed at anaphase I (Fig. 6D,J). Randomly distributed chromosomes aligned in metaphase II (Fig. 6E,K) and chromatids, after separation at anaphase II, were incorporated into polyads (Fig. 6F,L). The *Atmnd spo11-1* double mutant displayed the same meiotic defect as the *spo11-1* mutant, indicating that the function of *SPO11* is epistatic to *AtMND1*. In other words, the DNA fragmentation and chromosome entanglements seen in *Atmnd1* mutants stem from the activity of the Spo11-1 enzyme.

Axial element formation, sister chromatid cohesion and initiation of recombination appears normal in *Atmnd1* mutants

ASY1 is a meiosis-specific protein intimately associated with the chromosome axes during prophase I (Armstrong et al., 2002). SCC3 is a member of the cohesin complex and localizes along chromosome axes (Chelysheva et al., 2005). Both proteins behaved similarly in *Atmnd1* mutants compared with wild-type plants during the leptotene stage (data not shown) indicating that axial elements are formed normally and that sister-chromatid cohesion is established in *Atmnd1* mutants. In *Atmnd1* mutants, chromosome axes visualised with antibodies against ASY1 and SCC3, respectively, are not incorporated into an SC structure. We could not identify a pachytene stage in *Atmnd1* mutants as we did in the wild type (Fig. 7).

The chromosome fragmentation defect observed during meiosis in *Atmnd1* is compatible with a defect in the processing of DSBs that initiate recombination. We thus investigated the behaviour of RAD51, a key protein involved in mediating strand invasion during DSB repair. We immunolocalised the RAD51 protein on chromosome spreads and obtained results similar to those previously reported (Higgins et al., 2004). Numerous foci appeared at leptotene (Fig. 8A), probably corresponding to sites at which recombination had been initiated, and were observable during zygotene (Fig. 8B). The *Atmnd1* leptotene and zygotene stages were indistinguishable from wild-type cells, with respect to RAD51 focus formation (Fig. 8C,D), indicating that DSBs are made at a normal level.

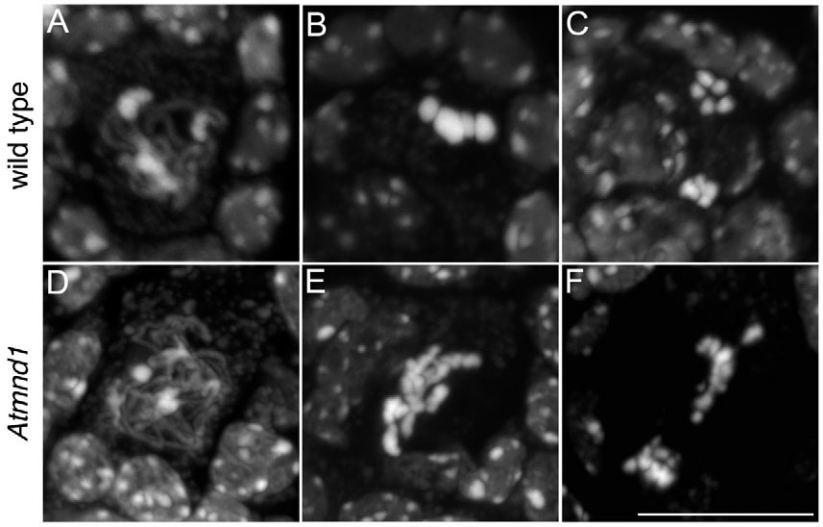

Fig. 4. Female meiosis is disrupted in *Atmnd1* mutants. Female meiosis in wild-type *A. thaliana*: (A) pachytene, (B) metaphase I, (C) anaphase I. Disrupted female meiosis in the *Atmnd1* mutant: (D) failed zygotene/pachytene, (E) metaphase-I-like stage with entangled chromosomes, (F) anaphase-I-like stage. Images show DAPI staining of the chromosomes. Bar, 10 μm.

AtMND1 interacts with AHP2 in a Y2H assay

AHP2 is the *Arabidopsis* homologue of Hop2 (Schommer et al., 2003), a yeast protein that interacts with Mnd1. We used a Y2H assay to test for a potential interaction between AtMND1 and AHP2. For this, we cloned the *AtMND1* cDNA into a yeast expression vector in-frame with a GAL4 DNA-binding domain, and the AHP2 cDNA in-frame with a GAL4 activator domain, and vice versa. Plasmids encoding DNA-binding domain and activator-domain fusion proteins were transformed together into yeast strain AH109 (Clontech). Control experiments were performed, by transforming AH109 with combinations of fusion-protein-containing vectors and empty vectors (Fig. 9). Whereas all plasmid combinations enabled yeast strain AH109 to grow on synthetic dropout (SD) medium selecting for the presence of the plasmids (SD –Leu/–Trp), only simultaneous transformation of plasmids encoding AtMND1 and AHP2 fusion proteins led to growth on selective plates (SD –Leu/–Trp/–His). We therefore conclude that AtMND1 interacts with AHP2.

Does MND1 have a role in somatic DNA repair?

Somatic expression of *MND1* has been observed in humans (Zierhut et al., 2004) and in *A. thaliana* (Fig. 1E) but not in yeast. Data from publicly accessible microarray databases (http://www.genevestigator.ethz.ch) show that *AtMND1* expression is upregulated approximately fivefold in response to genotoxic stress (*AHP2* is upregulated eightfold). These expression data point to a potential role of Mnd1 in somatic cells, presumably in DNA repair; this hypothesis has not yet been tested in mammals, as there is no mutant available. However, we investigated this issue in wild-type and *Atmnd1* mutant plants exposed to different genotoxic treatments. Mutant plants were germinated on plates containing different concentrations of hydroxyurea (HU). HU depletes the pool of dNTPs by inhibiting ribonucleotide reductase (RNR) (Krakoff et al., 1968), leading to a replication block and subsequent DNA DSBs. The length of developing roots in *Atmnd1* plants was monitored and compared with wild-type plants (Culligan et al., 2004). We could not detect any influence of the *Atmnd1* mutation on root growth on media

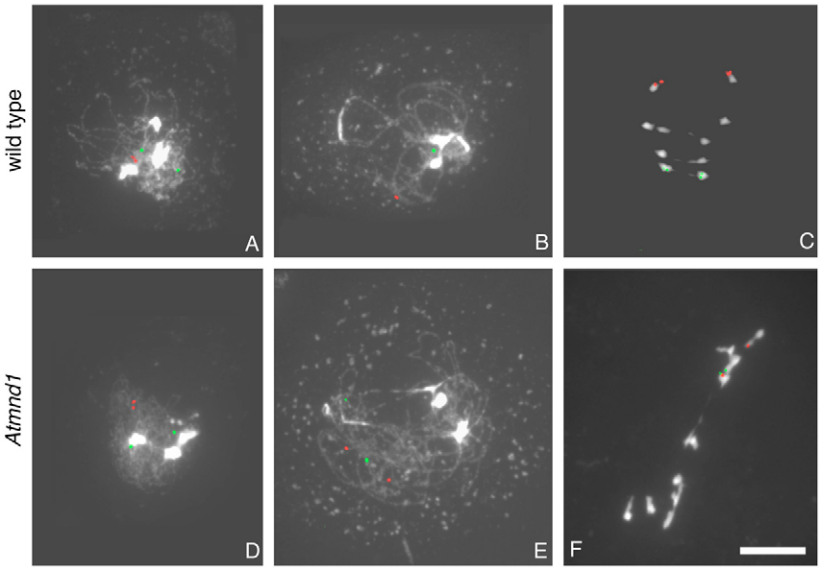

Fig. 5. FISH analysis of *Atmnd1* mutants reveals defects in pairing and chromosome disjunction. Preparations of wild-type (A-C) and *Atmnd1* (D-F) meiocytes were hybridised with FISH probes directed against an interstitial region of chromosome 1 (BAC F1N21, green) and a sub-telomeric region of chromosome 2 (BAC F11L15, red). (A,D) Zygotene stage, showing consistent association of sub-telomeric regions in wild-type and occasional association in *Atmnd1* cells. (B) Wild-type pachytene/diplotene transition with paired FISH probes. (E) *Atmnd1* pachytene-like stage with unpaired FISH signals. (C,F) Anaphase I with a regular distribution of chromosomes and FISH signals in wild-type meiocytes, as opposed to the irregular chromosome disjunction and DNA fragmentation in *Atmnd1* cells. Chromosomes are stained with DAPI. Bar, 10 μm.

plates with or without HU (data not shown). In addition, we germinated seedlings on media plates and exposed them to different doses of gamma-radiation to induce DSBs (Garcia et al., 2003). Exposure to gamma-radiation interfered with development to a similar extent in mutant and wild-type plants (data not shown). Furthermore, *Atmnd1* mutant plants had no growth defect when grown under normal conditions, contrary to the DNA-repair-deficient mutants *mre11* (Bundock and Hooykaas, 2002) and *rad50* (D. Vezon and M. Grelon, INRA, IJPB, Versailles, France, personal communication). Therefore, it was concluded that *AtMND1* has no essential role in somatic DNA repair, at least under the conditions tested.

Discussion

The model plant *Arabidopsis thaliana* is advantageous for studying meiosis, as it is amenable to molecular, cytological and genetic analysis. Furthermore, all stages of meiosis can be studied because mutations affecting meiotic DNA repair do not trigger a cell-cycle check point, in contrast to yeast and mammals. It is also emerging that model organisms such as *S. cerevisiae* do not reflect the full complexity of protein interactions in higher eukaryotes. Even though many proteins involved in meiotic DNA repair and recombination are conserved through evolution, their interaction partners, the chronology of their action and the impact of mutating them can be different. For example, the conserved protein Mre11 is necessary for DSB formation and processing in yeast, but in *A. thaliana* it is only necessary for the ensuing DNA processing after DSB formation (Puizina et al., 2004). Therefore, to fully understand the function of a meiotic protein such as Mnd1, and to reveal its interplay with other, potentially unknown protein factors, it is vitally important that it is characterised in different species.

The Hop2-Mnd1 complex is conserved in plants

In this study, we identified the *Arabidopsis MND1* homologue, *AtMND1*, and analysed its function through the isolation and characterisation of an *Atmnd1* mutant. This mutation leads to a strong male and female sterility phenotype that can be rescued by integrating a transgene carrying a wild-type copy of the *AtMND1* gene, confirming that the observed phenotype is caused by the *Atmnd1* mutation. In addition, we demonstrate that AtMND1 interacts with AHP2 (the *Arabidopsis* Hop2 homologue) in a Y2H assay, an interaction that has also been observed in yeasts and mammals (Petukhova et al., 2005; Saito et al., 2004; Tsubouchi and Roeder, 2002). The Mnd1-Hop2 complex is therefore conserved in higher eukaryotes.

AtMND1 is required for meiotic chromosome pairing and synapsis

As synapsis is severely disrupted, pachytene stages cannot be observed in either male or female *Atmnd1* meiocytes. Although it is possible that some synapsis initiation occurs in *Atmnd1*, synapsis does not advance to a substantial extent. ASY1, a protein associated with the chromosome axes (Armstrong et al., 2002; Caryl et al., 2000) and SCC3 (Chelysheva et al., 2005), a cohesion complex component, both localise to unsynapsed chromosomes at the right time, but extensive juxtapositioning of chromosome axes has not been observed with either marker. Furthermore, FISH probes associated with chromosomes 1 and 2, were not found in a paired configuration in *Atmnd1*, apart from early telomere pairing, that seems unaffected in *Atmnd1* mutants, but is not maintained during meiotic progression. Taken together, the existence of RAD51 foci, and the dependence of the observed meiotic aberrations on the SPO11-1 protein, demonstrate the existence of

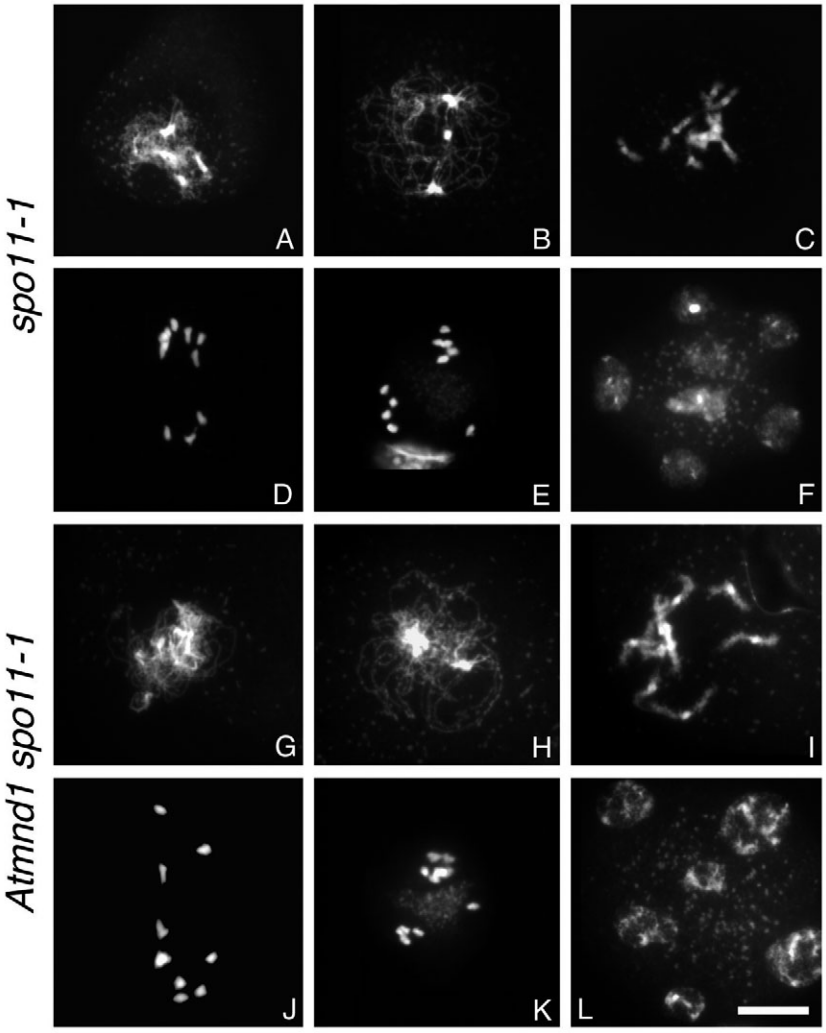

Fig. 6. Chromosome entanglement and fragmentation observed in *Atmnd1* mutants depends on SPO11-1. Comparison of meiotic progression in the *spo11-1* mutant (A-F) and in the *Atmnd1 spo11-1* double mutant (G-L). (A,G) Zygotene-like stage. No typical pachytene cells were detected, and only unsynapsed chromosomes were observed in the pachytene-like stage (B,H). In diakinesis (C,I), ten condensed univalents are visible. (D,J) Anaphase I. (E,K) Metaphase II. (F,L) Polyads. Chromosomes are stained with DAPI. Bar, 10 μm.

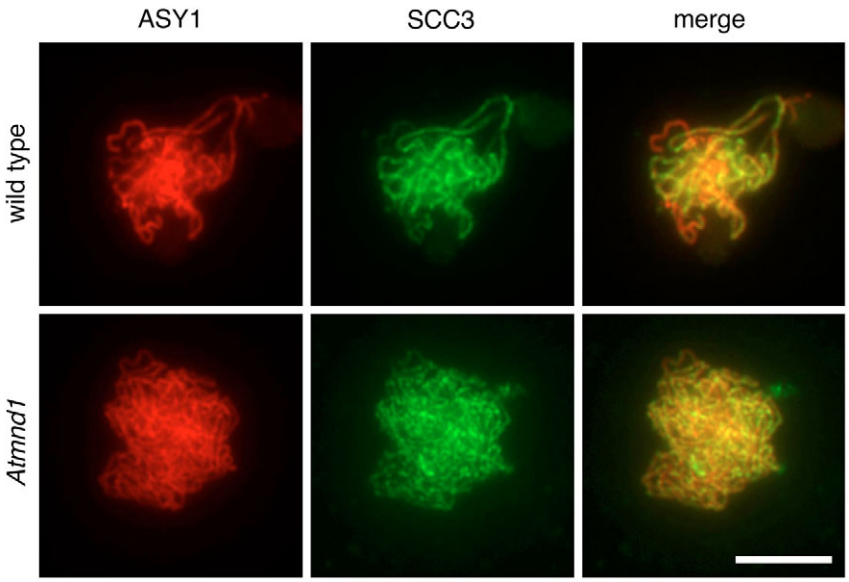

Fig. 7. Immunolocalisation of ASY1 and SCC3 in *Atmnd1* mutant plants. In *Atmnd1* mutants (lower panels), loading of the SCC3 cohesin protein (green) and of the axial-element associated ASY1 protein (red) is similar to that in wild-type plants (upper panels). However, no synapsis was observed in *Atmnd1* in contrast to wild-type cells. Bar, 10 μm.

chromatin breaks, a prerequisite for synapsis in *Arabidopsis*. Normal RAD51 focus formation has also been observed in *S. cerevisiae mnd1* and *hop2* mutants (Gerton and DeRisi, 2002; Tsubouchi and Roeder, 2002; Zierhut et al., 2004) as well in mouse *Hop2* mutants (Petukhova et al., 2003). The absence of homologous pairing and the subsequent observation of entangled multivalents are compatible with the existence of some kind of non-homologous interactions. This would be consistent with observations made in yeast *mnd1* and mouse *Hop2* mutants, which both have defects in SC formation.

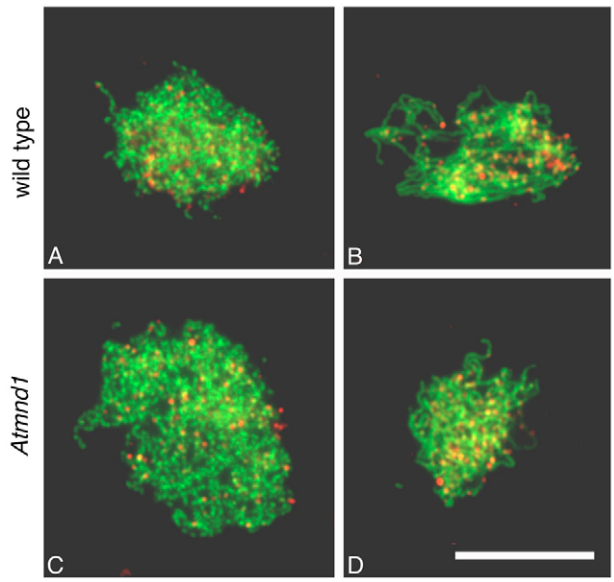

Fig. 8. Rad51 foci are formed normally in *Atmnd1* mutants. Comparison of RAD51 focus formation in wild-type (A,B) and *Atmnd1* mutant (C,D) plants. RAD51 foci (red) were observed in leptotene (A,C) of wild-type and of *Atmnd1* mutants cells and in zygotene (B) and failed zygotene stages (D) of wild-type and *Atmnd1* mutant cells, respectively. The abundance of RAD51 foci was similar in wild-type and *Atmnd1* mutant meiocytes. Immunolocalisation of ASY1 is represented in green. Bar, 10 μm.

Mouse *Hop2* mutants perform limited synapsis, most of it non-homologous (Petukhova et al., 2003). More extended synapsis occurs in *S. cerevisiae mnd1* mutants, but it is assumed to be non-homologous (Zierhut et al., 2004). This assumption is based on the similarity of SC extension in yeast *mnd1* and *hop2* mutants (Tsubouchi and Roeder, 2002) because synapsis in the latter mutant largely involves non-homologous chromosomes (Leu et al., 1998). Thus, it appears that yeast, mammals and plants share a common synapsis control pathway that depends on Mnd1-Hop2. It is interesting to note that the Mnd1-Hop2 complex is not conserved in all eukaryotes. *C. elegans* (Dernburg et al., 1998) and *D. melanogaster* (McKim et al., 1998), which differ in their initial steps of meiotic recombination (because Spo11 is not required for intact SC formation), lack the Mnd1-Hop2 complex (reviewed by Gerton and Hawley, 2005).

AtMND1 plays a crucial role in meiotic recombination

Mnd1 and Hop2 are required for meiotic recombination in yeast, but not for its initiation (Gerton and DeRisi, 2002; Tsubouchi and Roeder, 2002). Similarly, the mammalian HOP2 protein is not required for the initiation of DSBs, but only for their repair (Petukhova et al., 2003). Our results from *Arabidopsis thaliana*, are consistent with this view. Chromosome fragmentation and entanglements involving multiple chromosomes are observed during meiotic progression in *Atmnd1* mutants. Both fragmentation and chromosomal interconnections are only seen in the presence of SPO11-1, the central protein in DSB formation (Grelon et al., 2001). We propose that non-homologous interactions of chromosomes in meiotic prophase I lead to interconnected DNA masses, which can be observed at metaphase-I- and anaphase-I-like stages. Chromatin links that can be seen in metaphase-I-like stages support this view. Nevertheless, this hypothesis has to be proved by identifying non-homologous interactions. The majority of DSBs in *Atmnd1* mutants remain unrepaired, hence leading to chromosome fragmentation. This defect is comparable to yeast *mnd1* mutants, in which hyper-resected DSBs accumulate (Gerton and DeRisi, 2002; Tsubouchi and Roeder, 2002).

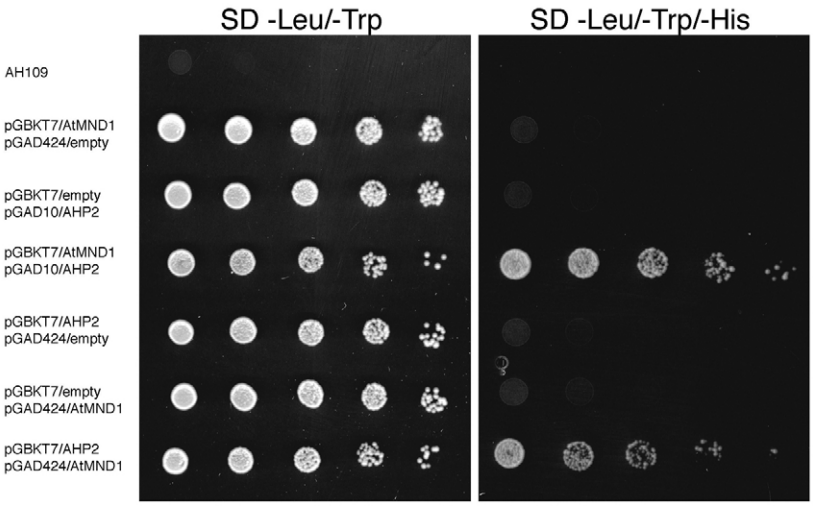

Fig. 9. AtMND1 and AHP2 interact in a yeast two-hybrid (Y2H) assay. Yeast strain AH109 was transformed with the indicated plasmids and grown on synthetic drop-out (SD) media lacking the amino acids leucine and tryptophan (SD –Leu/–Trp) or leucine, tryptophan and histidine (SD –Leu/–Trp/–His). Only the combination of plasmids containing AtMND1 fused to the GAL4-DNA binding domain and AHP2 fused to the GAL4 activator domain (pGBKT7/AtMND1, pGAD10/AHP2) or vice versa (pGBKT7/AHP2, pGAD424/AtMND1) enabled strain AH109 to grow on SD –Leu/–Trp/–His, demonstrating an interaction between AtMND1 and AHP2.

It has been proposed that the Mnd1-Hop2 complex cooperates with Dmc1 to promote stable-strand invasion (Gerton and DeRisi, 2002). Consistent with this proposal, Rad51 and Dmc1 physically interact with Hop2-Mnd1, and a purified Mnd1-Hop2 heterodimer stimulates the in vitro strand-invasion activity of Dmc1 (Chen et al., 2004; Petukhova et al., 2005). Nevertheless, Mnd1-Hop2 does not co-localise with Rad51 on meiotic chromosomes, arguing against a simple model in which the Mnd1-Hop2 complex directly promotes Dmc1 activity at the DSB site (Zierhut et al., 2004). Intriguingly, *Arabidopsis Atdmc1* and *Atmnd1* (and *ahp2*) mutants have different phenotypes. The *Atdmc1* mutation does not cause chromosome fragmentation, which would be reminiscent of a defect in DSB repair, but instead leads to the formation of univalents, which lack chiasmata (Couteau et al., 1999). It is thought that in the absence of AtDMC1, DSBs are repaired by the sister chromatid in *Arabidopsis*. In agreement with this conclusion, the additional depletion of RAD51 leads to DNA fragmentation in the *Atdmc1* mutant background, indicating that repair of DSBs depends on the presence of RAD51 in *Atdmc1* mutants (Siaud et al., 2004). Thus, it appears that in the absence of AtDMC1, repair occurs preferentially by the sister chromatid, whereas its presence promotes repair by the homologous chromosome. The *mnd1* and *ahp2/hop2* mutants in *Arabidopsis* and *S. cerevisiae* are unable to repair DSBs by using the sister chromatid. However, if the homologous chromosome is not present as a repair template, owing to disruption of SC lateral element proteins, such as Red1 or Hop1, *S. cerevisiae mnd1* mutants can repair DSBs via the sister chromatid (Zierhut et al., 2004). Further experiments are needed to resolve this issue in *Arabidopsis*. Other proteins involved in the control of inter-homologue bias during meiotic recombination are probably to be found in the group of RecA-related proteins and amongst accessory proteins of RecA-like proteins, such as the Dmc1 loading factor Tid1/Rdh54. Future efforts are needed to identify additional regulators and to decipher the relationship between RecA-like proteins and the AtMND1-AHP2 complex, and to understand how together they promote inter-homologue bias during meiotic recombination in plants.

Materials and Methods

Plant growth conditions, generation of a *Atmnd1/spo11-1* double mutant and plant transformation

All plants were germinated on media containing MS salts and 1% sucrose, and were transferred to soil after 3 weeks. Plants were grown at 22°C with a 16:8 hour light:dark photoperiod. Seeds of the *Atmnd1 A. thaliana* SALK_110052 line were obtained from the Nottingham *Arabidopsis* Stock Center (Nottingham, UK). Since *Atmnd1* mutants are sterile, the mutant allele was maintained by self-fertilization of heterozygous plants. *Atmnd1/spo11-1* double mutants were generated by crossing plants heterozygous for the *Atmnd1* mutation to plants heterozygous for an insertion in the *SPO11-1* gene (Grelon et al., 2001). Double mutants were identified by PCR of the F2 population, obtained by self-fertilising F1 plants heterozygous for both genes. Transformation of plants heterozygous for the *Atmnd1* mutation with pBIB-Hyg/gAtMND1, using *Agrobacterium tumefaciens* strain GV3101, was performed as described (Bechtold et al., 1993).

DNA analyses

DNA from flowers of individual plants was extracted according to Cocciolone and Cone (Cocciolone and Cone, 1993). DNA gel blot analysis of the *AtMND1* locus was performed with 1 μg genomic DNA digested with *Hin*dIII. A ^{32}P-labelled genomic fragment amplified by PCR with primers M1 and M4 was used as a probe for hybridisation. Plants were genotyped by PCR with two gene-specific primers and one primer specific for the left border of the T-DNA. Primers M2, M3 and LBa1 were used for the *AtMND1* locus. A 990 bp product was generated from wild-type alleles and a 1342 bp product from the Atmnd1 mutant allele. Primers SPO1, SPO2 and LB-BAR2 were used for the SPO11-1 locus, resulting in a 943 bp band and a ~500 bp product for wild-type and *spo11-1* alleles, respectively. For amplification of border regions, primers N610052U and LBSALK1 were combined in one reaction and N610052L and LBSALK1 in another reaction. Sequences of both PCR products were obtained (Genoscreen) and analysed with DNASSIST software (http://www.dnassist.org).

Construction of vectors

For construction of the complementing construct pBIB-Hyg/gAtMND1, BAC clone ATF19B15, obtained from ABRC (Columbus, Ohio), was digested with *Xmn*I and a 3806 bp genomic DNA fragment, harbouring the *AtMND1* gene and its putative promoter region, was ligated to the *Sma*I-digested plant binary vector pBIB-Hyg (Becker, 1990) and used for transformation.

For construction of the AtMND1-GAL4DB fusion protein vector, the *AtMND1* cDNA sequence, contained within plasmid U50561 (GenBank accession number BT005435), was amplified by PCR (Ex-Taq polymerase/TaKaRa, according to the manufacturer's instructions) with primers M1 and M4 and ligated into plasmid pCR2.1.TOPO (Invitrogen). The cDNA was released as a *Nde*I/*Bam*HI fragment from this vector and ligated into vector pGBKT7 (Clontech) digested with the same enzymes, giving rise to the Y2H vector pGBKT7/AtMND1. For construction of the AHP2-GALAD fusion protein, vector pGAD10 (Clontech) was digested with *Eco*RI, followed by Klenow treatment and subsequently digested with *Bam*HI. AHP2 cDNA (Schommer et al., 2003) was digested with *Xba*I, followed by Klenow treatment and subsequently digested with *Bam*HI. Ligation of these DNA fragments resulted in Y2H vector pGAD10/AHP2. For construction of the AHP2-GAL4DB fusion protein vector, *AHP2* cDNA, contained within plasmid pGAD10/AHP2, was amplified by PCR (Ex-Taq polymerase/TaKaRa) with primers AHP2_Ncodn and

AHP2_PstIup. The PCR fragment was digested with restriction enzymes *Nco*I and *Pst*I and ligated into vector pGBKT7 digested with the same enzymes, giving rise to Y2H vector pGBKT7/AHP2. For construction of the AtMND1-GAL4AD fusion protein vector, the *AtMND1* cDNA, contained within plasmid U50561, was amplified by PCR (Ex-Taq polymerase/TaKaRa) with primers Mnd1_EcoRIdn and MndI_PstIup. The PCR fragment was digested with restriction enzymes *Eco*RI and *Pst*I and ligated into vector pGAD424 (Clontech) digested with the same enzymes, giving rise to the Y2H vector pGAD424/AtMND1. All PCR generated *AtMND1* and *AHP2* fragments were sequenced to confirm error-free amplification. pGAD10 and pGAD424 are identical, and only differ in their multiple-cloning sites. Details of all primers used in this study can be found in supplementary material Table S1.

RNA extraction, RT-PCR and RACE

Total RNA was extracted from the indicated tissue using the TriReagent solution (Sigma, St Louis, MO), followed by DNA digestion (DNase, RNase free, 10 U/μl, Roche), phenol/chloroform extraction and RNA precipitation. 2 μg total RNA was used as a template for reverse transcription and generation of *AtMND1* and *ACTIN2/7* (At5g09810) cDNAs. Synthesis was primed by oligonucleotides M1 and Actin2.2 in one reaction and catalysed by AMV-RT as recommended by the manufacturer (Promega). One-tenth of the cDNA was used for PCR amplification with primers M1 and M4, and Actin2.1 and Actin2.2, respectively, applying standard PCR conditions. For rapid amplification of the 3′ end of the *AtMND1* cDNA ends (RACE), 5 μg total RNA from buds of wild-type plants was reverse-transcribed with AMV-RT (Promega) using primer AnchordT, as described above. 5 μl of this reaction was used as a template in a standard PCR reaction with primers Anchor and Mnd1_3RACE1. The PCR reaction was diluted 1:100 and 1 μl was used as a template for a second PCR, with nested primer Mnd1_3RACE2 and primer Anchor. The amplification product was gel-purified, ligated into PCR cloning vector pCR2.1TOPO (Invitrogen) and transformed into *E. coli*. Plasmids were isolated from five individual transformants and inserted PCR fragments were sequenced. For the RACE of the 5′ end of *AtMND1*, 3 μg RNA was reverse-transcribed using primer Mnd1_5RACE1 and M-MLV RT as recommended by the manufacturer (Promega). A polyA$^+$ tail was generated by incubating half of the cDNA reaction with TdT (MBI Fermentas), according to the manufacturer's manual. 5 μl of this reaction was used in a standard PCR reaction with primers AnchordT and Mnd1_5RACE1. The PCR reaction was diluted 1:100 and 1 μl was used for a second PCR using nested primers Anchor and Mnd1_5RACE2 in a standard PCR reaction. This PCR reaction was diluted 1:100 and 1 μl was used for the third PCR using primer Anchor and the nested primer Mnd1_5RACE3. The amplification product was analysed as described for the 3′ product.

Analysis of meiotic chromosomes

DAPI staining of male meiotic chromosomes was performed as described (Ross et al., 1996). Female meiotic chromosomes were observed as described (Motamayor et al., 2000).

Fluorescence in situ hybridisation (FISH)

The BAC clones F1N21 (chromosome 1) and F11L15 (chromosome 2) were obtained from ABRC (Columbus, Ohio), and used as probes. BAC DNA was isolated using the Qiagen Mini or Midi Prep kit and labelled by nick translation, following the manufacturer's instructions (Roche Diagnostics), with SpectrumGreen-dUTP (Vysis) and Cy3-dUTP (Amersham Pharmacia Biotech), respectively.

Chromosome spreads were prepared according to Armstrong et al. (Armstrong et al., 2001), except that whole flower buds were digested in 0.33% (w/v) cellulase 'Onozuka R-10' (Serva) and 0.33% (w/v) pectolyase (Sigma-Aldrich) for 90 minutes at 37°C, and meiocytes were left in 60% acetic acid at 45°C for a few seconds before re-fixation.

The FISH procedure was modified from Pedrosa et al. (Pedrosa et al., 2001) and Heslop-Harrison et al. (Heslop-Harrison et al., 1991) as follows. Preparations were pre-treated with RNAase for 30 minutes only and chromosomes were denatured in hybridization mix for 3 minutes at 73°C. Photographs were taken on a Zeiss Axioplan microscope (Carl Zeiss) equipped with a mono cool-view CCD camera (Photometrics, Tucson, AZ) and the IPLab spectrum software (IPLab, Fairfax, USA). Digital images were imported into Adobe Photoshop CS version 8 for final processing.

Fluorescent immunolocalisation

The immunolocalisation of the ASY1 and RAD51 proteins on chromosome spreads was carried out as described (Armstrong et al., 2002), except that whole buds, instead of isolated anthers, were used. No pre-blocking was applied. 10 μl anti-ASY1 (rabbit, 1:1000) and 10 μl anti-AtRAD51 (rat, 1:500), both diluted in blocking buffer (PBS + 0.1% Triton + 3% BSA), were used in combination. The secondary antibodies (20 μl anti-rat Cy3, Dianova/Szabo, 1:1000, and 20 μl anti-rabbit FITC, Sigma, 1:200 in blocking buffer) were applied consecutively and incubated at 37°C for 30 minutes. Slides were mounted in 2 μg/ml DAPI in Vectashield. Photographs were taken as described for FISH.

For ASY1 and SCC3 detection, chromosome spreads were prepared and immunofluorescence microscopy performed as described (Armstrong et al., 2002), using a Leica DMRXA2 fluorescence microscope. The ASY1 polyclonal antibody (Armstrong et al., 2002) was used at a working dilution of 1:500. The SCC3 antibody was described (Chelysheva et al., 2005) and used at a working dilution of 1:2000. Images were captured with a coolSNAP camera (Roper Scientific) driven by Openlab software (Improvision). These images were then processed with Adobe Photoshop 6.0 to improve image quality.

Yeast two-hybrid (Y2H) assay

Indicated combinations of plasmids were co-transformed into yeast strain AH109 (Clonetech) following the protocol for high-efficiency transformation of yeast (Burke et al., 2000). Following transformation, colonies were selected for the presence of the plasmids, inoculated in liquid synthetic drop-out (SD) media (lacking the amino acids leucine and tryptophan, with the exception of untransformed strain AH109, which was grown in YPAD), grown to saturation and plated onto SD media plates, lacking the indicated amino acids. SD media plates lacking the amino acids leucine, tryptophan and histidine (SD –Leu/–Trp/–His) were supplemented with 1 mM 3-Amino-1,2,4-triazol (Sigma). Serial 1:5 dilutions were made in water and 3 μl of each dilution was used to yield one spot. Plates were incubated at 30°C for two (SD –Leu/–Trp) or three (SD –Leu/–Trp/–His) days before taking pictures. The pictures were taken with a Nikon Coolpix 4500 digital camera and processed in Adobe Photoshop CS version 8.

We are grateful to Chris Franklin for sharing antibodies directed against ASY1 and RAD51. We thank Carla Schommer for helping constructing pGAD10/AHP2 and Franz Klein, Josef Loidl and Karel Riha for critical reading of the manuscript and/or stimulating discussions. This work was supported by a grant from the Austrian Science Foundation (P18036) to P.S. and by the Austrian Academy of Sciences (GMIGmbH).

References

Agarwal, S. and Roeder, G. S. (2000). Zip3 provides a link between recombination enzymes and synaptonemal complex proteins. *Cell* **102**, 245-255.

Alexander, M. P. (1969). Differential staining of aborted and nonaborted pollen. *Stain Technol*. **44**, 117-122.

Alonso, J. M., Stepanova, A. N., Leisse, T. J., Kim, C. J., Chen, H., Shinn, P., Stevenson, D. K., Zimmerman, J., Barajas, P., Cheuk, R. et al. (2003). Genome-wide insertional mutagenesis of Arabidopsis thaliana. *Science* **301**, 653-657.

Altschul, S. F., Madden, T. L., Schaffer, A. A., Zhang, J., Zhang, Z., Miller, W. and Lipman, D. J. (1997). Gapped BLAST and PSI-BLAST: a new generation of protein database search programs. *Nucleic Acids Res.* **25**, 3389-3402.

Armstrong, S. J., Franklin, F. C. and Jones, G. H. (2001). Nucleolus-associated telomere clustering and pairing precede meiotic chromosome synapsis in Arabidopsis thaliana. *J. Cell Sci.* **114**, 4207-4217.

Armstrong, S. J., Caryl, A. P., Jones, G. H. and Franklin, F. C. (2002). Asy1, a protein required for meiotic chromosome synapsis, localizes to axis-associated chromatin in Arabidopsis and Brassica. *J. Cell Sci.* **115**, 3645-3655.

Bechtold, N., Ellis, J. and Pelletier, G. (1993). In planta Agrobacterium mediated gene transfer by infiltration of adult Arabidopsis thaliana plants. *C. R. Acad. Sci. Paris Life Sci.* **316**, 1194-1199.

Becker, D. (1990). Binary vectors which allow the exchange of plant selectable markers and reporter genes. *Nucleic Acids Res*. **18**, 203.

Bergerat, A., de Massy, B., Gadelle, D., Varoutas, P. C., Nicolas, A. and Forterre, P. (1997). An atypical topoisomerase II from Archaea with implications for meiotic recombination. *Nature* **386**, 414-417.

Bundock, P. and Hooykaas, P. (2002). Severe developmental defects, hypersensitivity to DNA-damaging agents, and lengthened telomeres in Arabidopsis MRE11 mutants. *Plant Cell* **14**, 2451-2462.

Burke, D., Dawson, D. and Stearns, T. (2000). *Methods in yeast genetics. A Cold Spring Harbor Laboratory course manual.* Woodbury, CSHL Press.

Caryl, A. P., Armstrong, S. J., Jones, G. H. and Franklin, F. C. (2000). A homologue of the yeast HOP1 gene is inactivated in the Arabidopsis meiotic mutant asy1. *Chromosoma* **109**, 62-71.

Chelysheva, L., Diallo, S., Vezon, D., Gendrot, G., Vrielynck, N., Belcram, K., Rocques, N., Marquez-Lema, A., Bhatt, A. M., Horlow, C. et al. (2005). AtREC8 and AtSCC3 are essential to the monopolar orientation of the kinetochores during meiosis. *J. Cell Sci.* **118**, 4621-4632.

Chen, Y. K., Leng, C. H., Olivares, H., Lee, M. H., Chang, Y. C., Kung, W. M., Ti, S. C., Lo, Y. H., Wang, A. H., Chang, C. S. et al. (2004). Heterodimeric complexes of Hop2 and Mnd1 function with Dmc1 to promote meiotic homolog juxtaposition and strand assimilation. *Proc. Natl. Acad. Sci. USA* **101**, 10572-10577.

Cocciolone, S. M. and Cone, K. C. (1993). Pl-Bh, an anthocyanin regulatory gene of maize that leads to variegated pigmentation. *Genetics* **135**, 575-588.

Couteau, F., Belzile, F., Horlow, C., Grandjean, O., Vezon, D. and Doutriaux, M. P. (1999). Random chromosome segregation without meiotic arrest in both male and female meiocytes of a dmc1 mutant of Arabidopsis. *Plant Cell* **11**, 1623-1634.

Culligan, K., Tissier, A. and Britt, A. (2004). ATR regulates a G2-phase cell-cycle checkpoint in Arabidopsis thaliana. *Plant Cell* **16**, 1091-1104.

de Vries, F. A., de Boer, E., van den Bosch, M., Baarends, W. M., Ooms, M., Yuan, L., Liu, J. G., van Zeeland, A. A., Heyting, C. and Pastink, A. (2005). Mouse Sycp1 functions in synaptonemal complex assembly, meiotic recombination, and XY body formation. *Genes Dev*. **19**, 1376-1389.

Dernburg, A. F., McDonald, K., Moulder, G., Barstead, R., Dresser, M. and Villeneuve, A. M. (1998). Meiotic recombination in C. elegans initiates by a conserved mechanism and is dispensable for homologous chromosome synapsis. *Cell* **94**, 387-398.

Dresser, M. E., Ewing, D. J., Conrad, M. N., Dominguez, A. M., Barstead, R., Jiang, H. and Kodadek, T. (1997). DMC1 functions in a Saccharomyces cerevisiae meiotic pathway that is largely independent of the RAD51 pathway. *Genetics* **147**, 533-544.

Garcia, V., Bruchet, H., Camescasse, D., Granier, F., Bouchez, D. and Tissier, A. (2003). AtATM is essential for meiosis and the somatic response to DNA damage in plants. *Plant Cell* **15**, 119-132.

Gerton, J. L. and DeRisi, J. L. (2002). Mnd1p: an evolutionarily conserved protein required for meiotic recombination. *Proc. Natl. Acad. Sci. USA* **99**, 6895-6900.

Gerton, J. L. and Hawley, R. S. (2005). Homologous chromosome interactions in meiosis: diversity amidst conservation. *Nat. Rev. Genet.* **6**, 477-487.

Grelon, M., Vezon, D., Gendrot, G. and Pelletier, G. (2001). AtSPO11-1 is necessary for efficient meiotic recombination in plants. *EMBO J.* **20**, 589-600.

Henderson, K. A. and Keeney, S. (2004). Tying synaptonemal complex initiation to the formation and programmed repair of DNA double-strand breaks. *Proc. Natl. Acad. Sci. USA* **101**, 4519-4524.

Heslop-Harrison, J. S., Schwarzacher, T., Anamthawat-Jónsson, K., Leitch, A. R., Shi, M. and Leitch, I. J. (1991). In situ hybridization with automated chromosome denaturation. *Technique* **3**, 109-115.

Higgins, J. D., Armstrong, S. J., Franklin, F. C. and Jones, G. H. (2004). The Arabidopsis MutS homolog AtMSH4 functions at an early step in recombination: evidence for two classes of recombination in Arabidopsis. *Genes Dev.* **18**, 2557-2570.

Keeney, S., Giroux, C. N. and Kleckner, N. (1997). Meiosis-specific DNA double-strand breaks are catalyzed by Spo11, a member of a widely conserved protein family. *Cell* **88**, 375-384.

Krakoff, I. H., Brown, N. C. and Reichard, P. (1968). Inhibition of ribonucleoside diphosphate reductase by hydroxyurea. *Cancer Res*. **28**, 1559-1565.

Leu, J. Y., Chua, P. R. and Roeder, G. S. (1998). The meiosis-specific Hop2 protein of S. cerevisiae ensures synapsis between homologous chromosomes. *Cell* **94**, 375-386.

McKim, K. S., Green-Marroquin, B. L., Sekelsky, J. J., Chin, G., Steinberg, C., Khodosh, R. and Hawley, R. S. (1998). Meiotic synapsis in the absence of recombination. *Science* **279**, 876-878.

Mercier, R., Vezon, D., Bullier, E., Motamayor, J. C., Sellier, A., Lefevre, F., Pelletier, G. and Horlow, C. (2001). SWITCH1 (SWI1): a novel protein required for the establishment of sister chromatid cohesion and for bivalent formation at meiosis. *Genes Dev.* **15**, 1859-1871.

Motamayor, J. C., Vezon, D., Bajon, C., Sauvanet, A., Grandjean, O., Marchand, M., Bechtold, N., Pelletier, G. and Horlow, C. (2000). *Switch (swi1)*, an *Arabidopsis thaliana* mutant affected in the female meiotic switch. *Sex. Plant Reprod.* **12**, 209-218.

Nabeshima, K., Kakihara, Y., Hiraoka, Y. and Nojima, H. (2001). A novel meiosis-specific protein of fission yeast, Meu13p, promotes homologous pairing independently of homologous recombination. *EMBO J.* **20**, 3871-3881.

Okada, T. and Keeney, S. (2005). Homologous recombination: needing to have my say. *Curr. Biol*. **15**, R200-R202.

Page, S. L. and Hawley, R. S. (2003). Chromosome choreography: the meiotic ballet. *Science* **301**, 785-789.

Pâques, F. and Haber, J. E. (1999). Multiple pathways of recombination induced by double-strand breaks in Saccharomyces cerevisiae. *Microbiol. Mol. Biol. Rev.* **63**, 349-404.

Pedrosa, A., Jantsch, M. F., Moscone, E. A., Ambros, P. F. and Schweizer, D. (2001). Characterisation of pericentrometric and sticky intercalary heterochromatin in Ornithogalum longibracteatum (Hyacinthaceae). *Chromosoma* **110**, 203-213.

Petukhova, G. V., Romanienko, P. J. and Camerini-Otero, R. D. (2003). The Hop2 protein has a direct role in promoting interhomolog interactions during mouse meiosis. *Dev. Cell* **5**, 927-936.

Petukhova, G. V., Pezza, R. J., Vanevski, F., Ploquin, M., Masson, J. Y. and Camerini-Otero, R. D. (2005). The Hop2 and Mnd1 proteins act in concert with Rad51 and Dmc1 in meiotic recombination. *Nat. Struct. Mol. Biol.* **12**, 449-453.

Puizina, J., Siroky, J., Mokros, P., Schweizer, D. and Riha, K. (2004). Mre11 deficiency in Arabidopsis is associated with chromosomal instability in somatic cells and Spo11-dependent genome fragmentation during meiosis. *Plant Cell* **16**, 1968-1978.

Rabitsch, K. P., Toth, A., Galova, M., Schleiffer, A., Schaffner, G., Aigner, E., Rupp, C., Penkner, A. M., Moreno-Borchart, A. C., Primig, M. et al. (2001). A screen for genes required for meiosis and spore formation based on whole-genome expression. *Curr. Biol.* **11**, 1001-1009.

Ross, K. J., Fransz, P. and Jones, G. H. (1996). A light microscopic atlas of meiosis in Arabidopsis thaliana. *Chromosome Res*. **4**, 507-516.

Saito, T. T., Tougan, T., Kasama, T., Okuzaki, D. and Nojima, H. (2004). Mcp7, a meiosis-specific coiled-coil protein of fission yeast, associates with Meu13 and is required for meiotic recombination. *Nucleic Acids Res*. **32**, 3325-3339.

Schommer, C., Beven, A., Lawrenson, T., Shaw, P. and Sablowski, R. (2003). AHP2 is required for bivalent formation and for segregation of homologous chromosomes in Arabidopsis meiosis. *Plant J*. **36**, 1-11.

Schwacha, A. and Kleckner, N. (1997). Interhomolog bias during meiotic recombination: meiotic functions promote a highly differentiated interhomolog-only pathway. *Cell* **90**, 1123-1135.

Siaud, N., Dray, E., Gy, I., Gerard, E., Takvorian, N. and Doutriaux, M. P. (2004). Brca2 is involved in meiosis in Arabidopsis thaliana as suggested by its interaction with Dmc1. *EMBO J*. **23**, 1392-1401.

Tsubouchi, H. and Roeder, G. S. (2002). The Mnd1 protein forms a complex with hop2 to promote homologous chromosome pairing and meiotic double-strand break repair. *Mol. Cell. Biol*. **22**, 3078-3088.

Watanabe, Y. (2004). Modifying sister chromatid cohesion for meiosis. *J. Cell Sci.* **117**, 4017-4023.

Yamada, K., Lim, J., Dale, J. M., Chen, H., Shinn, P., Palm, C. J., Southwick, A. M., Wu, H. C., Kim, C., Nguyen, M. et al. (2003). Empirical analysis of transcriptional activity in the Arabidopsis genome. *Science* **302**, 842-846.

Yin, Y., Cheong, H., Friedrichsen, D., Zhao, Y., Hu, J., Mora-Garcia, S. and Chory, J. (2002). A crucial role for the putative Arabidopsis topoisomerase VI in plant growth and development. *Proc. Natl. Acad. Sci. USA* **99**, 10191-10196.

Zickler, D. and Kleckner, N. (1999). Meiotic chromosomes: integrating structure and function. *Annu. Rev. Genet.* **33**, 603-754.

Zierhut, C., Berlinger, M., Rupp, C., Shinohara, A. and Klein, F. (2004). Mnd1 is required for meiotic interhomolog repair. *Curr. Biol.* **14**, 752-762.

Table S1. Primer Sequences

M1	5′-CATATGTCTAAGAAACGGGGACTTTC-3′
M2	5′-GTGATCTGATATCTAGAGTCG-3′
M3	5′-AGGAATATACACATTGATACAGC-3′
M4	5′-CTAAGCTTCATCTTGTACTAGC-3′
SPO1	5′-CGTGTCCGAGCATAAAGCTTATGA-3′
SPO2	5′-CCCTTTGGTTTATCAGAGCTGCAT-3′
LB-BAR2	5′-TGTGCCAGGTGCCCACGGAATAGT-3′
LBSALK1	5′-CATCAAACAGGATTTTCGCC-3′
LBa1	5′-TGGTTCACGTAGTGGGCCATCG-3′
N610052U	5′-TACGTGTGCTTTTCACCAGA-3′
N610052L	5′-TGTTGCAACCTTTAAAACCAG-3′
AHP2_Ncodn	5′-TAGTCCATGGCTCCTAAATCGGATAAC-3′
AHP2_PstIup	5′-TATGCTGCAGTTACTGTCCTCGAGGCCTC-3′
Mnd1_EcoRIdn	5′-ATCGAATTCATGTCTAAGAAACGGGGACTTTC-3′
MndI_PstIup	5′-ATACCTGCAGCTAAGCTTCATCTTGTACTAGC-3′
Actin2.1	5′-CTGCCGCTGTTGTTTCTCCT-3′
Actin2.2	5′-CGTTGTAGAAAGTGTGATGCCA-3′
AnchordT	5′-GACCACGCGTATCGATGTCGAC$(T)_{16}$V-3′
Anchor	5′-GACCACGCGTATCGATGTCGAC-3′
Mnd1_3RACE1	5′-CTGGCAATCAACTTAGGAGTG-3′
Mnd1_3RACE2	5′-AGGGAAGAATCGGAGGAACG-3′
Mnd1_5RACE1	5′-AGCAACTTCAATTGCATTCCTC-3′
Mnd1_5RACE2	5′-TACCATCTCGTTCTTCAGATC-3′
Mnd1_5RACE3	5′-ACTCCTAAGTTGATTGCCAGC-3′